Bioimaging Hot Paper

DOI: 10.1002/ange.201400323

DNA Nanoflowers for Multiplexed Cellular Imaging and Traceable Targeted Drug Delivery**

*Rong Hu, Xiaobing Zhang, Zilong Zhao, Guizhi Zhu, Tao Chen, Ting Fu, and Weihong Tan**

Abstract: *We present a facile approach to make aptamer-conjugated FRET (fluorescent resonance energy transfer) nanoflowers (NFs) through rolling circle replication for multiplexed cellular imaging and traceable targeted drug delivery. The NFs can exhibit multi-fluorescence emissions by a single-wavelength excitation as a result of the DNA matrix covalently incorporated with three dye molecules able to perform FRET. Compared with the conventional DNA nanostructure assembly, NF assembly is independent of template sequences, avoiding the otherwise complicated design of DNA building blocks assembled into nanostructures by base-pairing. The NFs were uniform and exhibited high fluorescence intensity and excellent photostability. Combined with the ability of traceable targeted drug delivery, these colorful DNA NFs provide a novel system for applications in multiplex fluorescent cellular imaging, effective screening of drugs, and therapeutic protocol development.*

Simultaneous monitoring of multiple complex biochemical processes in living systems is particularly important for early disease diagnosis, therapy and biomedical studies, and it has attracted increasing attention in the past decade.[1] The use of molecular dyes with different emissions is one of the most attractive techniques for multifluorescent bioimaging by virtue of its high sensitivity, real-time spatial imaging and detection of targets in living systems. Of special interest are those dyes which exploit a single-excitation wavelength with resolvable multiple emission spectra.[2] Single excitation minimizes the complexity of fluorescent detection, thereby considerably simplifying the instrumentation requirements, while, at the same time, allowing a simultaneous excitation of all fluorophores used in one assay.[3] However, the number of available dyes that have single-wavelength excitation and distinguishable emission maxima is limited.[4] Moreover, organic dyes usually suffer from photobleaching, as well as poor water-solubility and membrane-permeability, defects which greatly limit their biological applications.[5] To address these issues, quantum dots (QDs) conjugated to biomolecules have been developed for long-term multicolor bioimaging,[6] but their cytotoxicity and complicated synthesis procedures have so far hampered their wide application.[7] By incorporating different dyes, FRET (fluorescent resonance energy transfer)-based multifluorescent silica nanoparticles have also been developed for multiplexed biomedical applications.[4,8] However, the use of silica nanoparticles will also result in dose-dependent cytotoxicity.[9] Therefore, the development of multifluorescent nanotags that are easy to synthesize, highly water-soluble, selective, biocompatible and photo-stable, capable of self-delivery, and sufficiently stable is highly desirable.

DNA is naturally water-soluble and biocompatible. Moreover, it is relatively simple to synthesize DNA with a commercial synthesizer. Recently, DNA has emerged as a favorable material for constructing DNA nanostructures with promising applications in biomedicine and biotechnology.[10] For example, using DNA as template, Qu et al. constructed a novel delivery and imaging platform for near infrared (NIR) light controlled non-invasive protein release.[10c] Thus, DNA nanostructures would seem to be a favorable platform for the construction of FRET-based multifluorescent nanotags for biomedical applications. Recently, the Mathies group has been developed FRET-based DNA structures that exploit to optimize the absorption and emission properties of the label. High FRET efficiency of the structures was achieved.[10d] However, conventional approaches for preparing DNA nanostructure typically depend on bottom-up assembly through Watson–Crick base-pairing between small DNA building blocks. This methodology possesses some intrinsic drawbacks, such as complicated design, the necessity of a large amount of DNA for bulk preparation, and dissociation that typically occurs due to denaturation or extremely low concentrations.

Rolling circle replication (RCR) can resolve these obstacles. RCR is an isothermal enzymatic reaction that can rapidly synthesize DNA, which has found wide uses in academic research and biotechnology.[11] Recently, our group reported the noncanonical self-assembly of hierarchical DNA nanoflowers (NFs) with densely packed DNA using RCR.[12] Long building blocks were generated by RCR, using only two DNA strands (one template and one primer). Without relying on Watson–Crick base-paring, NFs can be self-assembled through liquid crystallization of the resulting long building blocks. The obtained NFs exhibited exceptional stability under denaturing and biological environments. Furthermore, fluorescent tags can be enzymatically incorporated into NFs during RCR. These features make RCR-driven NFs assembly

[*] R. Hu, Prof. X. Zhang, Dr. Z. Zhao, Dr. G. Zhu, Dr. T. Chen, T. Fu, Prof. W. Tan
Molecular Science and Biomedicine Laboratory, State Key Laboratory for Chemo/Bio-Sensing and Chemometrics, College of Biology, and College of Chemistry and Chemical Engineering, Collaborative Research Center for Chemistry and Molecular Medicine, Hunan University
Changsha 410082 (China)
E-mail: tan@chem.ufl.edu

[**] This work was supported by the National Key Scientific Program of China (2011CB911000), NSFC grants (21325520, 21327009, 21221003, J1210040, 21177036, 21135001), and China National Instrumentation Program 2011YQ03012412.

Supporting information for this article is available on the WWW under http://dx.doi.org/10.1002/anie.201400323.

a highly desirable strategy for assembling DNA nanostructures for biomedical applications.

Herein, we report a facile approach for making aptamer-conjugated FRET-nanoflowers by RCR for single-excitation multiplexed imaging and traceable targeted drug delivery. Aptamers, which are single-stranded oligonucleotides, provide an attractive alternative to antibodies for recognizing multiple trace biomarkers or cancer cells in complex biological samples.[13] In this study, fluorescein (FAM), cyanine 3 (Cy3), and 6-carboxyl-X-rhodamine (ROX) were simultaneously incorporated into NFs via chemically modified deoxynucleotides, including FAM-dUTP, Cy3-dUTP, and ROX-dUTP, during RCR reaction. When the ratio of these fluorophores was varied in this enzymatic reaction, FRET-mediated emission signatures could be tuned such that NFs would exhibit colors under one single-wavelength excitation. As a result, these DNA nanoflowers not only exhibited multiple and extremely bright fluorescence signals under a single-wavelength excitation, but they also represented a target-specific and biocompatible drug delivery platform. The FRET NFs also allow for a large Stokes shift, which benefits applications in complex biological milieu.

Multicolor FRET DNA nanoflowers are generated through RCR. The long linear single-stranded DNA encoding complementary sequences of the aptamer are prepared first (Figure 1). Since NF assembly is independent of template sequences, all aptamer-complementary sequences can be used in our strategy.[12] In this study, aptamers sgc8[14] and MUC 1[15] were chosen to construct our model NFs. Aptamer sgc8 specifically recognizes PTK7 over-expressed on various types of cancer cells.[14] Aptamer MUC 1 targets an important class of tumor surface markers expressed on a broad range of epithelial cancer cells.[15] The nick in the circular DNA was chemically closed with a T4 DNA ligase. The closed circular DNA template was then used in the subsequent rolling DNA replication. The Φ29 polymerase which is commonly used in multiple displacement amplification was used for fabrication of our DNA NFs. The nucleotide adenosine (A) was strategically spaced along the DNA template, providing regular positions to attach the multidye-modified dUTPs on the replicated product. It has been reported that dye-modified dUTPs can be recognized by many DNA polymerases, including Φ29,[16] enabling their incorporation into NFs. Accordingly, FAM, Cy3 and ROX were chosen to build the FRET cascades required to implement our multifluorescent imaging platform. These dyes were chosen on the basis of good spectral overlap required by FRET (Figure S1 in the Supporting Information). The RCR template was designed to construct multifunctional NFs (sequence shown in Table S1; predicted structure in Figure S2) such that the resulting elongated complementary ssDNA would be decorated with a series of aptamers and drug-loading sites for doxorubicin (Dox). Therefore, optimal targeted imaging and delivery could be realized by developing multifunctional DNA NFs according to the specific characteristics of cancer cells.

The above RCR-generated elongated ssDNAs can work as building blocks to assemble NFs. The enzymatic reaction was first verified using gel electrophoresis. The results

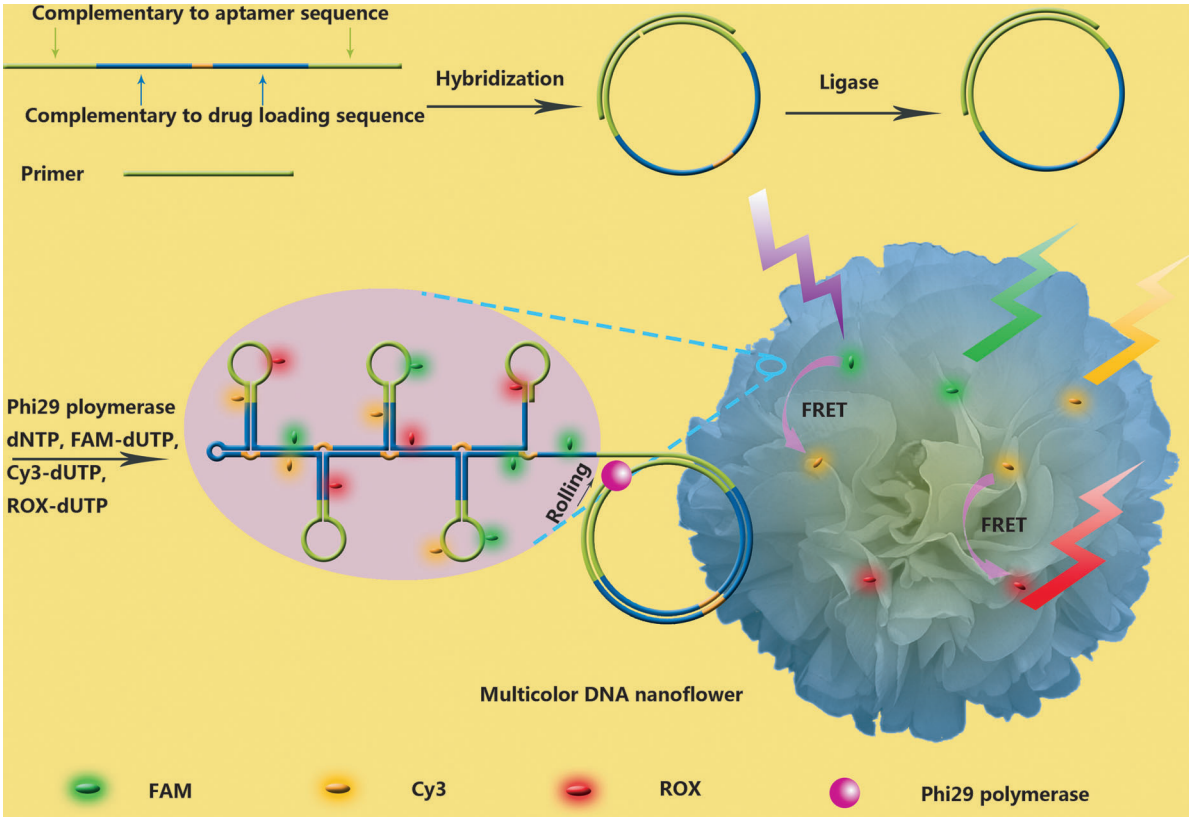

Figure 1. Bioassisted, sequence-independent self-assembly of multicolor FRET DNA nanoflowers NFs.

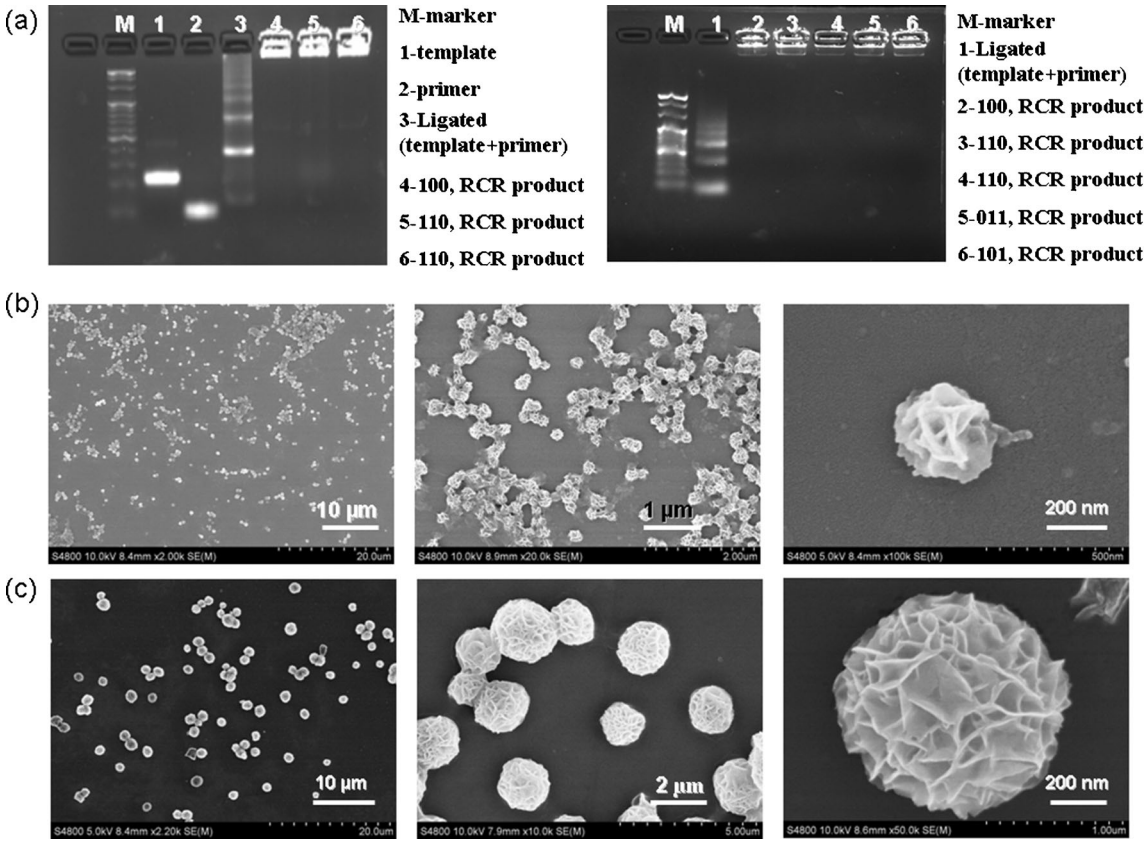

Figure 2. a) Agarose gel (2%) electrophoresis image indicating the elongation of DNA through RCR. Left: sgc 8-incorporated DNA NFs; right: MUC 1-incorporated DNA NFs. b) SEM image of DNA NFs (**RCR$_{15}$**, 001); c) SEM images of the hierarchal NFs from **RCR$_{30}$** with diameters of approximately 2 μm.

indicated the successful generation of long DNA strands through RCR (Figure 2a). In order to simplify the notation, the three colored samples prepared at FAM/Cy3/ROX = 1:0:0, FAM/Cy3/ROX = 1:1:0, and FAM/Cy3/ROX = 1:1:1 are hereinafter denoted as 100, 110, and 111, and the RCR products obtained after reaction for n hours were denoted as **RCR$_n$**. The morphology of DNA NFs was evaluated by scanning electron microscopy (SEM). As seen in Figure 2b, the diameter of the sgc8-incorporated ROX DNA nanoflower (**RCR$_{15}$**, 001) after 15 h is above 250 nm with petal-like structures, and the DLS result revealed an average radius of 140 ± 10 nm (Figure S3). The DNA NFs with two (**RCR$_{15}$**, 011) or three dyes (**RCR$_{15}$**, 111) have the similar "flower" structures (Figure S4,5). Our results represent the first to build monodisperse FRET DNA nanomaterials with diameters as small as 250 nm through RCR. Moreover, the NF size could be tuned to a few micrometers (e.g., 2 μm) by increasing the reaction time to 30 h (Figure 2c, Figures S6 and S7). Gel electrophoresis was also used to verify enzymatic reaction for the MUC 1 aptamer (Figure 2a). The diameter of MUC 1 aptamer-conjugated nanoflowers was then characterized by SEM (Figures S8 and S9). All of the NFs, including those doped with single, dual, and even triple fluorophores, displayed as monodisperse spherical "flowers" in SEM imaging.

In order to confirm the formation of multicolored fluorescent FRET DNA NFs, the fluorescence spectra of DNA NFs doped with FAM, Cy3 and ROX were investigated. The introduction of single FAM, Cy3 or ROX dye did not change the excitation and emission spectra (Figure 3a). As shown in Figure 3b, the simultaneous appearance of the emissions of three dyes excited at 488 nm was observed. DNA NFs (111) co-doped with triple dyes showed three peaks at 520, 565, and 610 nm, which are attributed to the emissions of FAM, Cy3, and ROX, respectively. The decreased emission of FAM and drastically increased emission of ROX demonstrates efficient FRET between dyes in the particle. The fluorescence emission shape varies with the doping ratios, which indicate that a finely controllable fluorescent signal is easily achieved. Using single FAM DNA NFs (100) and FAM-Cy3 co-doped NFs (110), we calculated a transfer efficiency (E) of 33% from the spectral properties of the fluorophores. We have also calculated the Förster distance (R_0) for the dyes pairing in DNA NFs. The R_0 values for FAM-Cy3, FAM-ROX and Cy3-ROX were 6, 3.7 and 5.6 nm, respectively, and their corresponding average separation distances were 4.8, 3 and 4 nm, respectively. Moreover, FRET could be better illustrated by exciting samples (a) and (b) using the maximum absorption wavelength of FAM at 494 nm. One can observe that sample (b) showed a higher fluorescent intensity at 565 nm than that of sample (a) (Figure S10).

Single-particle brightness is a key characteristic in fluorescence imaging, and distinguishable bright colors were clearly detected, as shown in Figure S11. To further examine

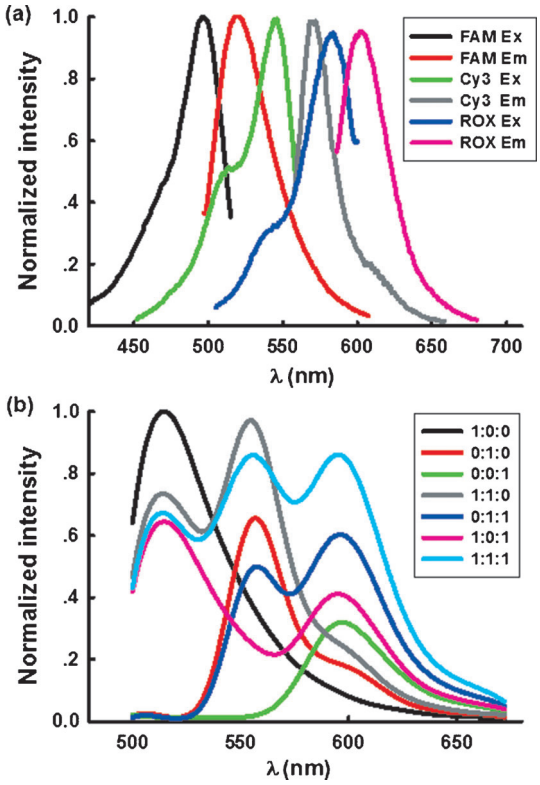

Figure 3. a) Excitation and emission spectra of DNA NFs doped with FAM, Cy3, or ROX only; b) Fluorescence emission spectra of NF samples encapsulated with one, two, or three types of fluorophores excited at 488 nm.

the efficiency of FRET, NFs co-doped with different dyes were investigated by single-particle fluorescence imaging at 488 nm argon-ion laser excitation. As seen in Figure S11, the results obtained agreed with those from the fluorescence spectra. By varying the different ratios of each dye with single, dual and triple dyes, the FRET-mediated NP emission signatures could be adjusted, resulting in NPs that exhibited different colors. Five kinds of nanoflowers doped with FAM, Cy3 and ROX with different ratios were mixed together and excited with a 488 nm argon-ion laser, and distinguishable bright colors were clearly and simultaneously observed (Figure S12).

To determine whether any dyes were leaking from NFs, the particles were subjected to ultrasound and centrifugation treatment. After storage for 36 h, the fluorescence intensity showed little change (Figure S13), and remained physically stable for one month. The above experiment was repeated three times, clearly indicating that the dye molecules which were covalently incorporated to the DNA matrix were very stable and did not readily leak from the NFs. To assess the stability of NFs under nuclease treatment, NFs were incubated with DNase I for 24 h. The result shown that DNA NFs were exceptionally resistant to nuclease treatment with DNase I concentration up to 5 U mL^{-1} (Figure S14). Moreover, no noticeable change was observed in the fluorescence intensity of the FAM-DNA NFs after successive illumination experiments over 1 h in duration with a UV source (300 W mercury lamp) (data not shown). The photostability, combined with the excellent biostability of NFs, provide the basis for these FRET-NFs to be applied in long-term bioimaging, especially in complex biological environment.

To demonstrate the suitability of NFs for multicolor applications with single-wavelength excitation, we used NFs with different ratios of each dye in multicolor confocal imaging. The cells incubated with single FAM-doped NFs have only green emission of FAM (Figure S15, top panels), while cells with FAM and Cy3 co-doped NFs show green and orange two emissions simultaneously (Figure S15, bottom panels). Similar results were also seen with MUC 1 aptamer incorporated multicolored DNA NFs (**RCR$_{15}$**, 110), a MUC1-postive human breast cancer cell line (MCF-7; MUC 1^{+}) was used. Under the excitation wavelength of 488 nm, two emissions attributed to FAM and Cy3 could be simultaneously observed based on the formation of FRET, while only the emission of Cy3 could be detected using the excitation wavelength of Cy3 at 543 nm (Figure 4). Thus, it is plausible that a multicolor bioimaging system induced by FRET can be obtained by varying the ratio between different fluorophores. Moreover, when the diameter of the FAM NFs (**RCR$_{30}$**, 100) increased to 2 μM, cellular entry was prevented, suggesting that the larger size and strong net negative surface charge of DNA NFs probably prevents cellular internalization (Figure S16). A co-localization study was also carried out. The result demonstrated that the DNA NFs resided in the lysosomes (Figure S17). We further monitored the fluorescent DNA NFs in target living cells in situ. The continuous enhancement of fluorescence intensities indicated that the DNA NFs possessed the ability for in situ imaging in living cells (Figure S18). Taken together, these results show that the

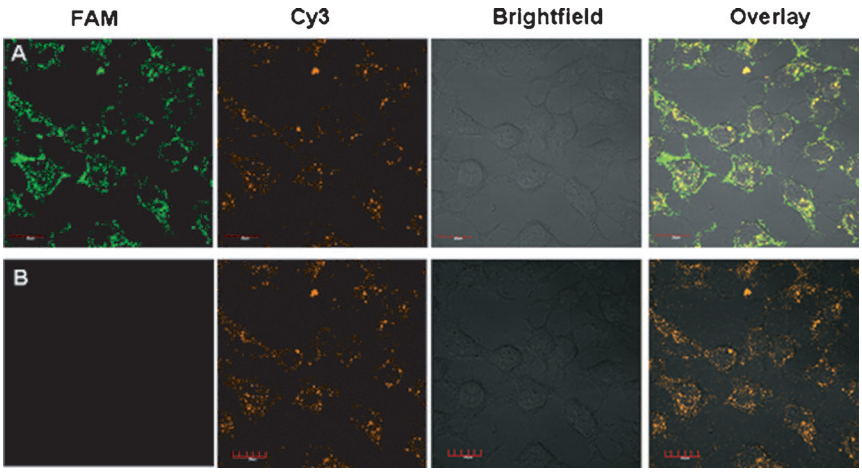

Figure 4. Confocal fluorescence images of living MCF-7 cells incubated with MUC 1-incorporated multicolored DNA NFs (**RCR$_{15}$**, 110) at 37 °C for 2 h. A and B were acquired under 488 and 543 nm argon-ion laser excitation, respectively.

multifluorescent NFs ($\mathbf{RCR_{15}}$) are able to efficiently penetrate cells for simultaneous monitoring.

Targeting of specific cells can be achieved by targeting certain membrane proteins. To accomplish this, we chose aptamer sgc8 as a model. In order to determine if the conjugated aptamer still preserves its binding affinity and specificity, the binding of NFs ($\mathbf{RCR_{15}}$, 100) toward target (CEM and HeLa) and control (Ramos) cancer cells was studied using flow cytometry. As shown in Figure S19, a large shift was observed for CEM cells (Figure S19a) and HeLa cells (Figure S19c) treated with the NFs ($\mathbf{RCR_{15}}$, 100), but no significant shift was observed for Ramos cells (Figure S19b). To further test whether DNA NFs could be used for specific labeling of live cells, sgc8-incorporated NFs which were used for labeling were incubated with cells and then washed. As indicated in Figure S20, after 30-minute incubation with DNA NFs, they were specifically bound with CEM cells at 4 °C. Since labeling with DNA NFs was shown to be specific, this approach can also be extended to specifically label multiple different proteins or cell types simultaneously to visualize their interactions in living cells and in whole organisms in situ.

Having demonstrated the feasibility of our DNA NFs for multicolor imaging, we investigated their feasibility for tracing drug transport. To load Dox into NFs, Dox and sgc8 aptamer-functionalized NFs ($\mathbf{RCR_{15}}$, 100) were mixed and incubated for 24 h, followed by centrifugation to remove free Dox in the supernatant. The confocal images in Figure 5 show overlapping green ($\mathbf{RCR_{15}}$, 100) and red (Dox) fluorescence signals corresponding to the cellular co-localization of FAM-NFs ($\mathbf{RCR_{15}}$, 100) and Dox, respectively. In HeLa cells treated with Dox-loaded FAM-NFs for 24 h, Dox was found to accumulate in the nucleus. The results confirm that these multicolor NFs have potential application as fluorescently traceable drug carriers.

We further evaluated the in vitro selective cytotoxicity of anticancer drugs transported by the DNA NFs. Specifically, target CEM and HeLa cells, as well as nontarget Ramos cells, were all treated with free Dox and NF-Dox ($\mathbf{RCR_{15}}$, 001) in equivalent drug concentrations. Results indicated that free Dox showed dose-dependent cytotoxicity in both CEM cells and Ramos cells. In contrast, only in target CEM and HeLa cells (Figure S21) did Dox transported by sgc8-NFs induce dose-dependent cytotoxicity comparable to that of free Dox. DNA nanomaterials have attracted tremendous interest, in large part owing to their good biocompatibility, which was also verified by an MTS assay that showed negligible inhibition of proliferation in cancer cells (CEM and Ramos) (Figure S22). The ability of Dox delivered by NFs to induce selective cytotoxicity in target cells indicates the potential of NFs to be applied in targeted drug delivery.

In conclusion, we report the first synthesis of multicolor DNA NFs by a single-wavelength excitation by rolling circle replication. They are uniform and exhibit high fluorescence intensity and excellent photostability. In contrast to conventional DNA nanostructures which demand many DNA strands, only two strands, one template and one primer, are required for NF assembly. Also, NF assembly is independent of template sequences, avoiding the otherwise complicated design of DNA base-pairing for conventional nanostructure assembly. The RCR products could carry concatameric aptamers, thus avoiding complex bioconjugation procedures. Therefore, all aptamer-complementary sequences can be tuned according to specific applications in our strategy. By optimizing the amount of dye molecules in FRET NFs, the emission spectra can be tuned so that only the longest-wavelength dye will exhibit significant fluorescence at a short-wavelength excitation. Furthermore, these FRET-NFs can also be used for targeted drug delivery. We believe that these NFs represent a promising tool for use in a variety of biomedical applications.

Received: January 12, 2014
Published online: April 17, 2014

Keywords: aptamers · DNA nanoparticles · drug delivery · multicolor imaging · single-wavelength excitation

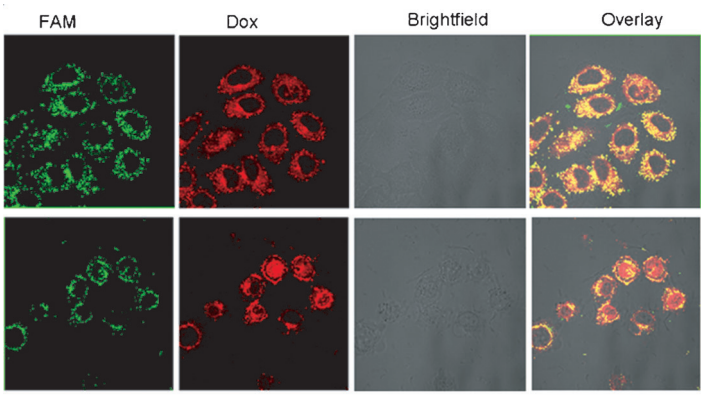

Figure 5. Confocal fluorescence images of Dox distribution in HeLa cells treated with Dox-loaded DNA NFs (RCR_{15}, 100) for 2 h (top panels) and 24 h (bottom panels).

[1] a) B. N. Giepmans, S. R. Adams, M. H. Ellisman, R. Y. Tsien, *Science* **2006**, *312*, 217 – 224; b) K. A. Giuliano, P. L. Post, K. M. Hahn, D. L. Taylor, *Annu. Rev. Biophys. Biomol. Struct.* **1995**, *24*, 405 – 434; c) C. J. Bettinger, R. Langer, J. T. Borenstein, *Angew. Chem.* **2009**, *121*, 5512 – 5522; *Angew. Chem. Int. Ed.* **2009**, *48*, 5406 – 5415.

[2] D. M. Shcherbakova, M. A. Hink, L. Joosen, T. W. J. Gadella, V. V. Verkhusha, *J. Am. Chem. Soc.* **2012**, *134*, 7913 – 7923.

[3] X. Chen, M. C. Estévez, Z. Zhu, Y. Huang, Y. Chen, L. Wang, W. Tan, *Anal. Chem.* **2009**, *81*, 7009 – 7014.

[4] L. Wang, W. Tan, *Nano Lett.* **2006**, *6*, 84 – 88.

[5] K. E. Sapsford, L. Berti, I. L. Medintz, *Angew. Chem.* **2006**, *118*, 4676 – 4704; *Angew. Chem. Int. Ed.* **2006**, *45*, 4562 – 4589.

[6] a) M. Han, X. Gao, J. Z. Su, S. Nie, *Nat. Biotechnol.* **2001**, *19*, 631 – 635; b) J. K. Jaiswal, H. Mattousi, J. M. Mauro, S. M. Simon, *Nat. Biotechnol.* **2003**, *21*, 47 – 51; c) H. Yao, Y. Zhang, F. Xiao, Z. Xia, J. Rao, *Angew. Chem.* **2007**, *119*, 4424 – 4427; *Angew. Chem. Int. Ed.* **2007**, *46*, 4346 – 4349.

[7] Y. Li, Y. Zhou, H. Wang, S. Perrett, Y. Zhao, Z. Tang, G. Nie, *Angew. Chem.* **2011**, *123*, 5982 – 5986; *Angew. Chem. Int. Ed.* **2011**, *50*, 5860 – 5864.

[8] D. Lu, J. Lei, L. Wang, J. Zhang, *J. Am. Chem. Soc.* **2012**, *134*, 8746 – 8749.

[9] a) M. Chen, A. Von Mikecz, *Exp. Cell Res.* **2005**, *305*, 51 – 62; b) W. S. Lin, Y. W. Huang, X. D. Zhou, Y. F. Ma, *Toxicol. Appl. Pharmacol.* **2006**, *217*, 252 – 259.

[10] a) T. Zhou, P. Chen, L. Niu, J. Jin, D. Liang, Z. Li, Z. Yang, D. Liu, *Angew. Chem.* **2012**, *124*, 11433 – 11436; *Angew. Chem. Int. Ed.* **2012**, *51*, 11271 – 11274; b) E. Cheng, Y. Xing, P. Chen, Y. Yang, Y. Sun, D. Zhou, L. Xu, Q. Fan, D. Liu, *Angew. Chem.* **2009**, *121*, 7796 – 7799; *Angew. Chem. Int. Ed.* **2009**, *48*, 7660 – 7663; c) L. Zhou, Z. Chen, K. Dong, M. Yin, J. Ren, X. Qu, *Adv. Mater.* **2014**, *26*, 2424 – 2430 d) J. Ju, C. Ruan, C. W. Fuller, A. N. Glazer, R. A. Mathies, *Proc. Natl. Acad. Sci. USA* **1995**, *92*, 4347 – 4351.

[11] a) J. B. Lee, J. Hong, D. K. Bonner, Z. Poon, P. T. Hammond, *Nat. Mater.* **2012**, *11*, 316 – 322; b) W. Zhao, C. H. Cui, S. Bose, D. Guo, C. Shen, W. P. Wong, K. Halvorsen, O. C. Farokhzad, G. S. L. Teo, J. A. Phillips, D. M. Dorfman, R. Karnik, J. M. Karp, *Proc. Natl. Acad. Sci. USA* **2012**, *109*, 19626 – 19631.

[12] G. Zhu, R. Hu, Z. Zhao, K. R. Williams, Z. Chen, X. Zhang, W. Tan, *J. Am. Chem. Soc.* **2013**, *135*, 16438 – 16445.

[13] X. Fang, W. Tan, *Acc. Chem. Res.* **2009**, *43*, 48 – 57.

[14] D. Shangguan, Y. Li, Z. Tang, Z. C. Cao, H. W. Chen, P. Mallikaratchy, K. Sefah, C. J. Yang, W. Tan, *Proc. Natl. Acad. Sci. USA* **2006**, *103*, 11838 – 11843.

[15] a) M. Brayman, A. Thathiah, D. D. Carson, *Reprod. Biol. Endocrinol.* **2004**, *2*, 4 – 15; b) M. Chang, C. Yang, D. Huang, *ACS Nano* **2011**, *5*, 6156 – 6163.

[16] a) D. Shalon, S. J. Smith, P. O. A. Brown, *Genome Res.* **1996**, *6*, 639 – 645; b) J. P. Anderson, B. L. Reynolds, K. Baum, J. G. Williams, *Nano Lett.* **2010**, *10*, 788 – 792.